

## NAWTEC16-1919

### Recycling of Municipal Solid Waste Ash through an Innovative Technology to Produce Commercial Zeolite material of High Cation Exchange Capacity

Maysson Sallam, PhD<sup>1\*</sup>, Robert P. Carnahan<sup>2</sup>, Abl Zayed<sup>3</sup>, and Sermin Sunol<sup>4</sup>

<sup>1</sup>Camp Dresser and McKee, CDM, West Palm Beach, FL, USA

<sup>2,3</sup>Department of Civil and Environmental Engineering, Faculty, University of South Florida, Tampa, Florida, USA

<sup>4</sup>Department of Chemical Engineering, Faculty, University of South Florida, Tampa, Florida, USA

\*Corresponding author, e-mail sallamm@cdm.com, fax +561-689-9713.

#### ABSTRACT

Municipal solid waste ash (MSW ash) samples, obtained from a local incinerator in Florida, were converted via a chemical process into zeolite material. The conversion process was performed by applying a two step treatment. The ash samples were fused at 550°C under alkaline conditions and then the fused ash samples were treated hydro-thermally at 60 °C and 100°C for different periods. This innovative technology involves adjusting the SiO<sub>2</sub>/Al<sub>2</sub>O<sub>3</sub> ratio of the ash from 13.9 to 2.5 by adding sodium aluminates and by using a solid to liquid ratio of 10. The fusion step formed sodium silicate and sodium aluminum silicate phases. These phases acted as precursors to the formation of zeolite A. Zeolite A was successfully formed within the ash matrix when samples were fused and SiO<sub>2</sub>/Al<sub>2</sub>O<sub>3</sub> was adjusted. The maximum cation exchange capacity, CEC, was measured by using ammonium acetate solution. The CEC of the produced zeolitic ash material has increased significantly from 17 meq/100g for non-treated ash up to 212 meq/100g for the treated ash. The cation exchange capacity of the produced zeolite ash material is close to that available from commercial zeolite materials which have a CEC of 245meq/100g. Zeolite A formation within the ash matrix increased the potential of using the ash as an adsorbent for industrial and environmental applications including ammonia removal from waste water or any other similar application that involves cation exchange.

#### 1. INTRODUCTION

In the United States, about 225 million tons of municipal solid waste are generated annually. One third of this waste is either recycled or composted. Landfilling or incineration manages about 150 million tons of municipal solid wastes. Incineration is becoming a favorable option for many reasons including problems associated with landfilling, excellent volume reduction, energy recovery and revenues gained. Landfilling is facing increasing opposition by both regulatory and public agencies due to their drastic effect on the environment; in consequence, landfills in the United States decreased from 8,000 in 1988 to 1,858 in 2001. In the United States, about 14% of generated waste, 86,000 tons, is incinerated yearly. Though incineration results in 70-90 % volume reduction of waste, a significant portion remains as ash. The remaining ash portion is usually divided into bottom ash fraction which accounts for 90% of the produce ash and fly ash fraction which accounts for only

10% of the total ash portion. Concerns still exist for landfilling of the remaining ash. This generated interest in treating and reusing the ash. To date, only 5% of the produced ash is being utilized in the United States. The majority of application has been in construction applications.

Only recently, an innovative technology proposed chemical conversion of the ash to produce zeolites material. The possibility of successfully producing zeolite from the ash is contributed to the fact that the ash has considerable fraction of silica and alumina, which are the primary elements required for building zeolite structure. This type of conversion is expected to increase the adsorption capacity of the ash due to the formation of zeolite minerals such as zeolite X, P and A within the ash matrix, which in consequence increases the potential of using the ash as an adsorbent in so many different applications. The investigation on zeolite synthesis process from municipal solid waste ash is still in its early stages and there is little work that has been done so far to address zeolite formation from municipal solid waste ash. None of the previous work addressed the formation process comprehensively to answer many questions regarding the types of zeolite that could be possibly produced, the optimization of the process, mechanism and theory of the formation, and the possibility of modeling the synthesis process. This paper addresses the formation process of zeolite A from MSW ash.

#### 2. THEORY AND MECHANISM OF ZEOLITE SYNTHESIS

The mechanism of zeolite formation from MSW ash has not been investigated in the previous literatures. However, recent theory for Zeolite synthesis from coal ash has been provided by many authors and can be used for comparison purposes in this study since coal ash has a similar composition as MSW ash. Murayama et. al., 2002 and 2003, suggested a theory for zeolites formation from coal ash and was based on the formation of amorphous aluminosilicate gel on the solid particles under high alkaline conditions followed by crystallization of zeolite due to the reaction between the gel and the alkali or dissolved species in the mother liquor solution. This theory concluded for zeolite synthesis process using the hydrothermal method and it was based on type of zeolite produced as a function of time and by following the growth trend as observed in scanning electron microscopy images. Similarly, Molina and Poole, 2004,

explained zeolite formation to be due to the reaction between the alkali metal in solution and the dissolved silicate and aluminates species that were released from the aluminosilicate gel which was formed during the fusion step. They argued that the formation of the gel in the fusion step enhanced zeolite formation because the gel provided enough active forms of silicates and aluminates species that initiate zeolite nucleation.

### 3. EXPERIMENTAL

An ash sample, obtained from a local incinerator in Florida, was milled until 80% of the sample passed through 425-micrometer sieve. The milled ash sample was then divided in smaller portions and each was fused at 550°C in a muffle furnace for 3 hours under alkaline conditions using 1.5, 2.5 and 3.5 normal solutions of sodium hydroxide. Then both fused and non-fused samples were placed in 250 ml-sealed bottles and placed in an oven for hydrothermal treatment at 60 and 100 °C for 2, 6, 24, and 72 hours. Inductively Coupled Plasma, ICP, analysis of the ash showed that the SiO<sub>2</sub>/Al<sub>2</sub>O<sub>3</sub> ratio in the ash is 13.9, this ratio was reduced to 2.5 by adding sodium aluminates while maintaining the solid / liquid ratio fixed at 1/10. The types of zeolitic materials produced were evaluated using X-Diffraction (Cu-α radiation, 45 KV, 40 mA, and scan range from 2 to 600 at step size of 0.05). Zeolite A formation and gel formation stages were studied by scanning electron microscope (SEM). The cation exchange capacity of the zeolites was determined using the sodium acetate method.

### 4. RESULTS AND ANALYSIS

#### 4.1 OPTIMIZATION OF ZEOLITE A FORMATION PROCESS

Optimizing SiO<sub>2</sub>/Al<sub>2</sub>O<sub>3</sub> ratio and forming the silicate precursors, such as sodium silicate and sodium aluminum silicate, are important steps in forming zeolite A (F. Polak, 1971; S. Yamazaki and K. Tsutumi, 2000; and N. N. Feoktistova and S. P. Zhdanov, 1996). As shown in Table 1, a SiO<sub>2</sub>/Al<sub>2</sub>O<sub>3</sub> molar ratio of 13.9 is considered too high for zeolite A to form. Therefore, this ratio was reduced to 2.5 by adding sodium aluminates, which increases the concentration of aluminum in the tetrahedral structure. This is necessary to initiate nucleation of zeolite A and reduce the effect of hydroxyl ion attack on the formed nuclei (S. Bosnar and B. Subotic, 1999). Fusing the ash in the first step causes dissolution of the quartz and glass and formed sodium silicate and sodium aluminum silicate precursors to the production of zeolite A during the hydrothermal treatment. Table 2 shows different phases formed as a result of subjecting the ash to fusion at 550 °C for 3 hours using sodium hydroxide concentration of 1.5, 2.5 and 3.5 normality, respectively. As shown in Table 2, the fusion step did actually result in production of phases that could be of important in directing the reaction toward the formation of different zeolite phases. Fusing the ash at 1.5 N produced a sodium aluminum silicate phase that could work as precursor to zeolite formation. Fusion of the ash at 2.5 and 3.5 produced sodium silicate phase which is an important precursor to zeolite formation. An additional phase was formed at 3.5N that was identified to be unnamed zeolite. Quartz phase was not detected when ash was fused at 2.5N and it

**Table 1 Chemical composition of ash shown for major and minor elements.**

Elemental Oxide	Weight % as Oxide	Molar %
Al <sub>2</sub> O <sub>3</sub>	7.86	0.08
SiO <sub>2</sub>	67.20	1.115
CaO	12.51	0.22
Fe <sub>2</sub> O <sub>3</sub>	6.47	0.04
MgO	1.01	0.03
Na <sub>2</sub> O	5.43	0.09
K <sub>2</sub> O	0.61	0.0065
MnO	0.05	0.0007
CuO	0.08	0.001
TiO <sub>2</sub>	6.72	0.08
ZnO	0.49	0.006
PbO	2.46	0.0201
Loss on ignition = 10.7 %		

**Table 2 Phases produced as a result of subjecting the ash to fusion at 550 °C for 3 hours.**

Fusion Conditions	Fusion at 550 °C for 3 hours		
	1.5N	2.5N	3.5N
Hydroxide concentration , N			
Phases formed	%	%	%
SiO <sub>2</sub>	31.6	-	4.6
CaCO <sub>3</sub>	2.1	-	-
CaCO <sub>3</sub> +Sodium silicate (Na <sub>2</sub> SiO <sub>3</sub> )	-	8.0	15.14
Sodium alumina silicate, (NaAlSiO <sub>4</sub> )	18.3	-	-
Sodium alumina silicate hydrate, Unnamed zeolita (Na <sub>2</sub> Al <sub>2</sub> Si <sub>1.68</sub> .O <sub>7.76</sub> .1.73H <sub>2</sub> O)	-	-	10.9
Sodium carbonate hydrate, (Na <sub>2</sub> CO <sub>3</sub> .H <sub>2</sub> O)	48	34.5	69.3
Sodium carbonate, (Na <sub>2</sub> CO <sub>3</sub> )	-	22.9	-
Sodium nitrate , (NaNO <sub>2</sub> )	-	34.5	-

was considerably low at 3.5N. Calcite phase was detected regardless of what fusion condition is used.

#### 4.2 X-RAY DIFFRACTION ANALYSIS

Mineralogical compositions for the untreated and treated samples were evaluated primarily by X-Ray diffraction technique using Cu-κ<sub>α</sub> radiation and crystalline titanium oxide (IV), TiO<sub>2</sub> (< 5 micron, 99.9+%), as an internal standard. Figure 1 shows the results of X-ray analysis for the combined non-treated ash sample. As shown in Figure 1, calcite and quartz are the major crystalline phases present in the ash. The hump noticed in the X-Ray pattern indicates the presence of amorphous materials, which are likely to be the glass portion

which is abundant in the ash as was noticed in the physical examination of the ash. Figure 2 shows representative X-ray diffraction pattern for fused ash showing the formation of zeolite A precursors sodium aluminum silicate and sodium silicate. Figure 3 shows the X-Ray diffraction pattern for a representative sample showing the formation of zeolite A for the samples that were subjected to fusion followed by hydrothermal treatment. Hydrothermal treatment for non-fused samples did not show zeolite A formation at any condition investigated and therefore were not included in the results. The lack of formation of zeolite A for the non-fused hydrothermally treated samples could be due to the absence of the silicate precursors required for zeolite A nucleation.

### 4.3 SCANNING ELECTRON MICROSCOPY ANALYSIS

The morphology and crystal size of the non-treated and treated ash were studied by using Scanning Electron Microscopy Images. Gel and zeolite formation stages and mechanism of formation were assisted through observations of the SEM images. Figures 4-10 present scanning electron microscopy, SEM, images for original and treated samples at different studied conditions. Figure 4 shows a typical image for the ash particles with sharp non-homogenous morphology. Figure 5A presents the SEM images for fused samples at 1.5N where it shows the formation of clusters of alumina silicate with flaky structure. These clusters acted as a precursor to zeolite A formation. Figure 5B and 5C show SEM images of the formation of zeolite A and unnamed zeolite at 6 and 24 hours. At 72 hours, only unnamed zeolite was formed as shown in figure 5D. The zeolite A crystals sizes ranged between 0.4-0.56  $\mu\text{m}$  when sample was treated at 1.5N at 100  $^{\circ}\text{C}$ .

Figures 6-A, 6-B and 6-C show SEM images for cubic zeolite A as it formed at 1.5N at 60  $^{\circ}\text{C}$  for 6,24 and 72 hours. The crystal sizes for zeolite A ranged between 0.5-0.62  $\mu\text{m}$ . Figure 7-A shows SEM image of the formation of alumina silicate clusters with rose like surface structure for fused ash at 2.5N where Figures 7-B, 7-C and 7-D show SEM images for zeolite A formation at 100  $^{\circ}\text{C}$  for 6, 24 and 72 hours, respectively. Zeolite A crystal sizes were between 0.7-1.2  $\mu\text{m}$ . Figures 8-A, 8-B and 8-C show SEM images for zeolite A formation at 6,24 and 72 hours for fused ash at 2.5N at 60  $^{\circ}\text{C}$ . Zeolite A crystal sizes were 1.1-1.6  $\mu\text{m}$  in this case. Figure 9-A shows aluminosilicate cluster formation for the fused sample at 3.5 N that also has a rose like surface structure. Figures 9-B, 9-C and 9-D show zeolite A formation at 6,24 and 72 hours for fused ash at 3.5N at 100  $^{\circ}\text{C}$ , respectively. Zeolite A crystal sizes were formed in the range between 0.54-0.81  $\mu\text{m}$ . Figures 10-A, 10-B and 10-C show zeolite A formation at 6,24 and 72 hours, respectively, for fused ash at 3.5N at 60  $^{\circ}\text{C}$ . Zeolite A crystal sizes were in the range of 0.7 – 0.9  $\mu\text{m}$ .

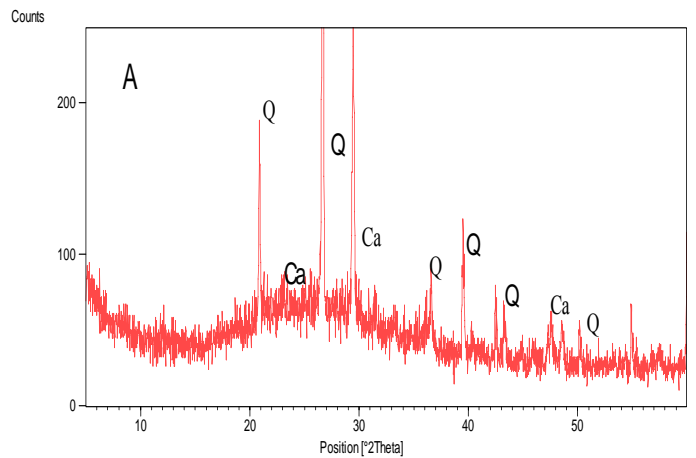


**Fig. 1 X-ray diffraction patterns for non-treated ash sample. Q: Quartz, Ca: Calcite.**

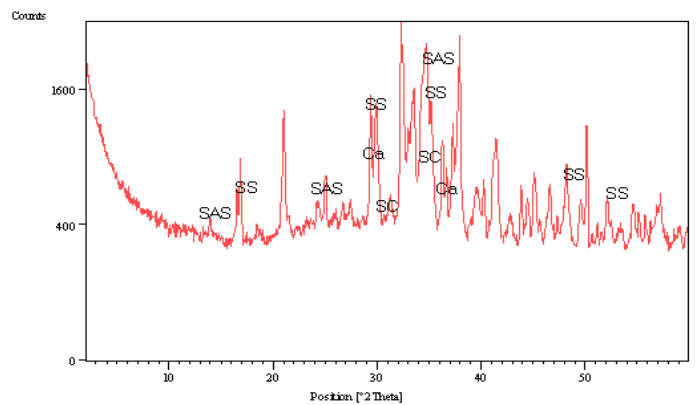


**Fig. 2 Results of X-Ray for Fused ash SAS: Sodium Aluminum silicate, SS: Sodium Silicate, A: Zeolite A, Zk-14: Zeolite Zk-14, Q: Quartz, Ca: Calcite.**

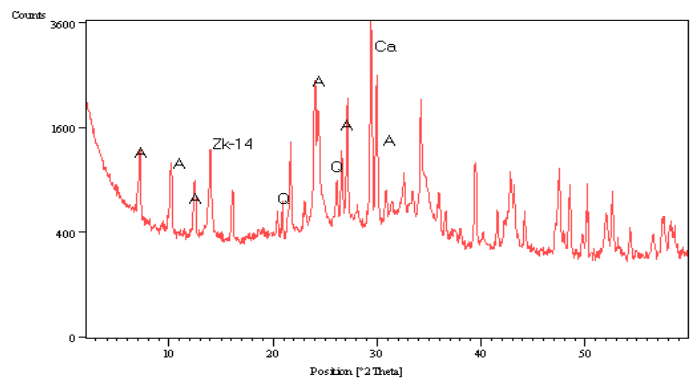


**Fig. 3 Results of X-Ray for hydrothermal treatment for the fused samples, A: Zeolite A, Zk-14: Zeolite Zk-14, Q: Quartz, Ca: Calcite.**

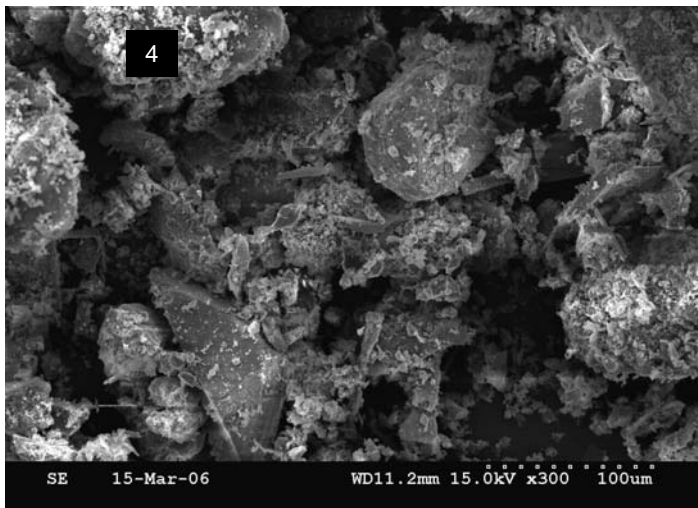


**Fig. 4** SEM image for original ash showing sharp non homogenous components.

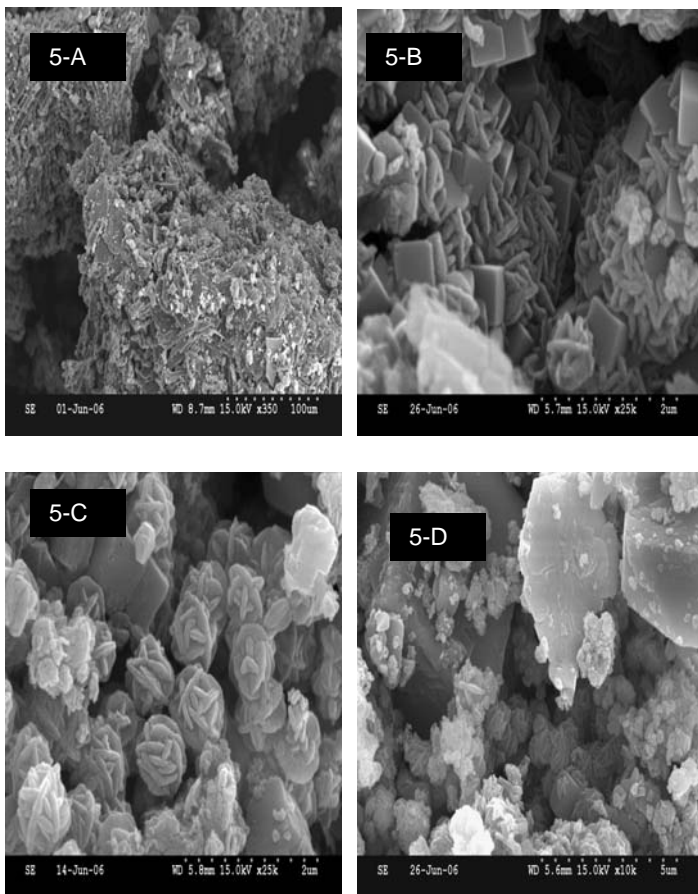
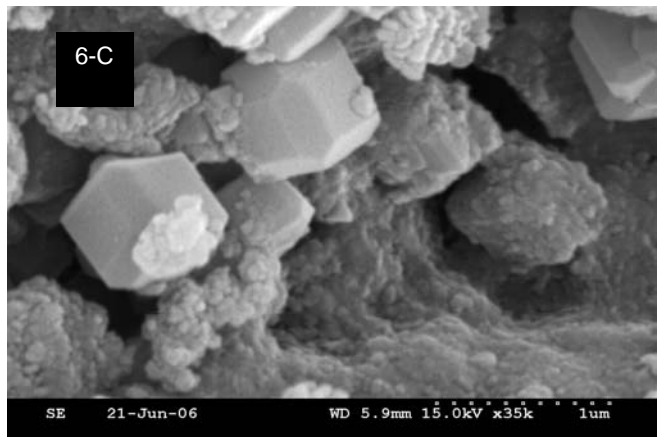
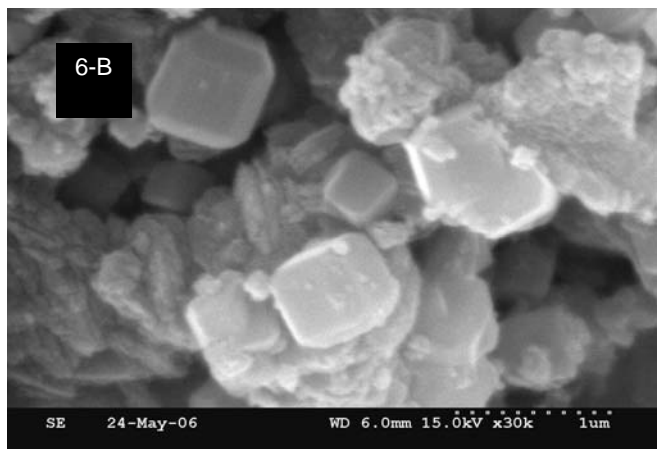
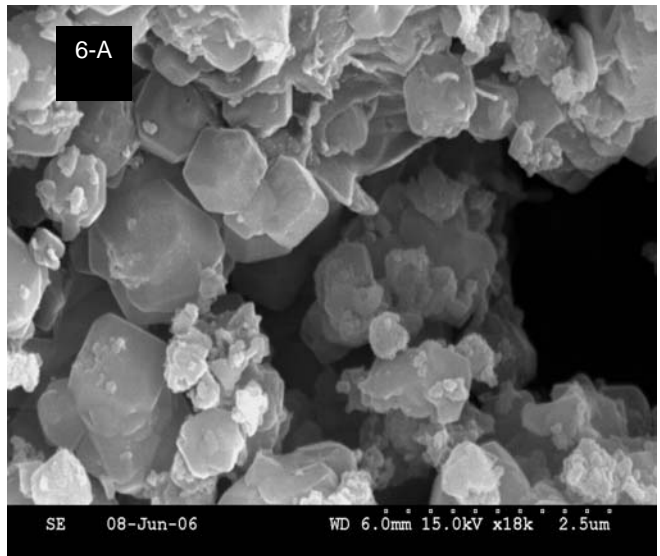


**Fig. 5** Fused ash at 1.5 N at 100 °C. A) Fused ash B) 6 hours showing Unnamed Zeolite C) 24 hours showing Cubic Zeolite A D) 72 hours, Unnamed Zeolite and Gibbsite large crystal.

**Fig. 6** Fused ash at 1.5N at 60 °C. Zeolite A formation at different crystallization periods. A) 6 hours B) 24 hours and C) 72 hours.

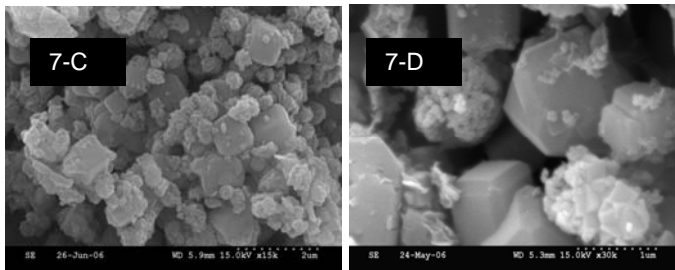
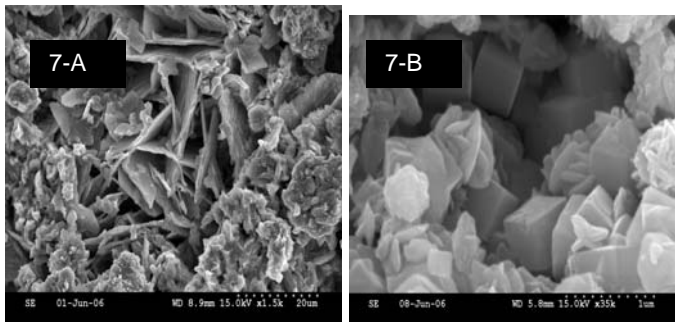


**Fig. 7 Fused ash at 2.5N at 100 °C. A) Fused ash B) 6 hours, Zeolite A and zeolite ZK-14 C) 24 hours, cubic Zeolite A and Unnamed Zeolite D) 72 hours, Zeolite A and Sodalite.**

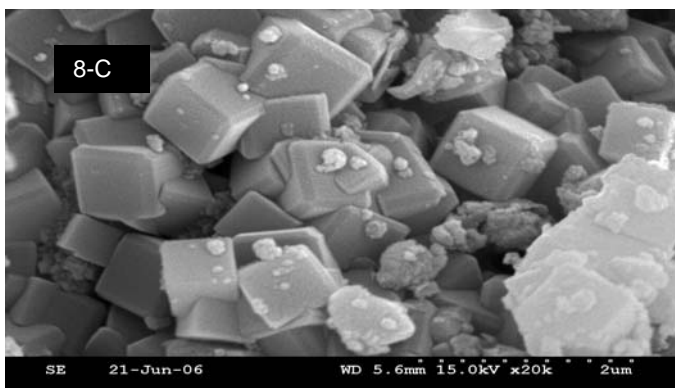
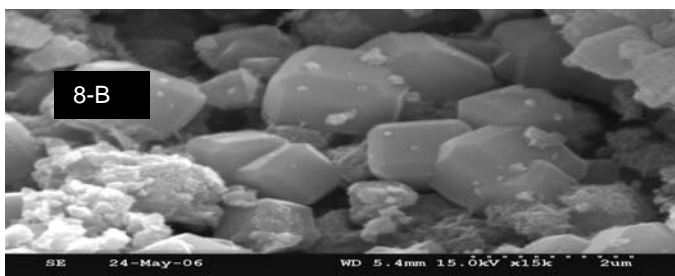
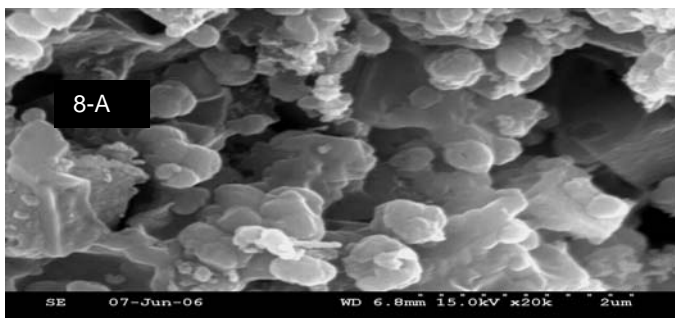


**Fig. 8 Fused ash at 2.5N at 60 °C. Zeolite A formation at different crystallization periods. A) 6 hours B) 24 hours and C) 72 hours.**

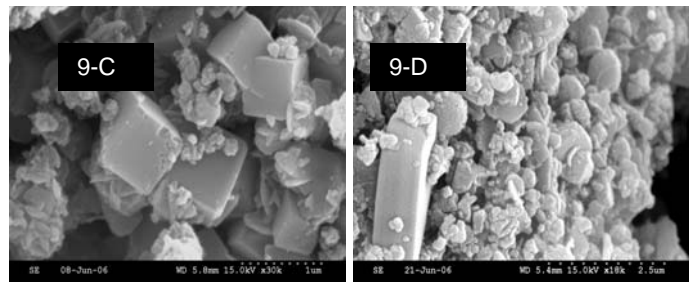
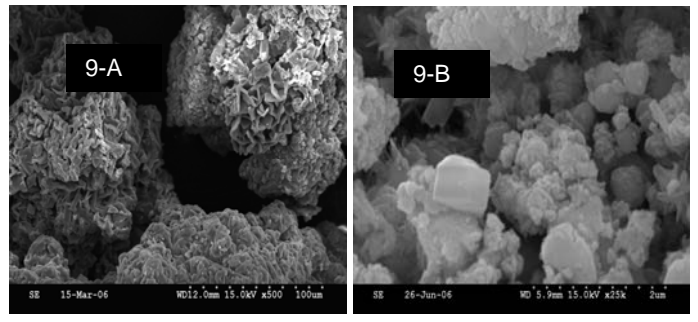


**Fig. 9 Fused ash at 3.5N at 100 °C. A) Fused ash B) 6 hours, Zeolite A and Unnamed zeolite C) 24 hours, cubic Zeolite A D) 72 hours, Sodalite.**

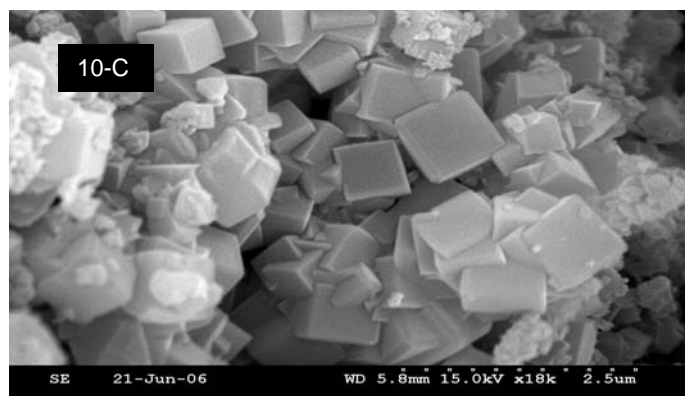
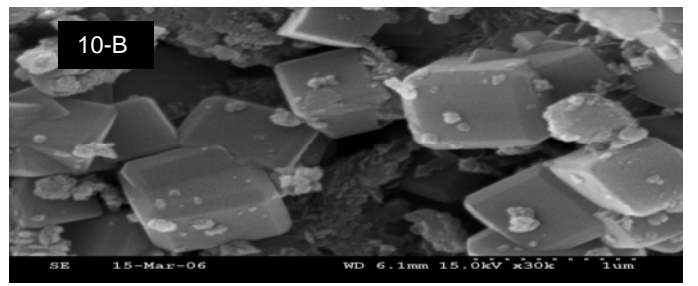
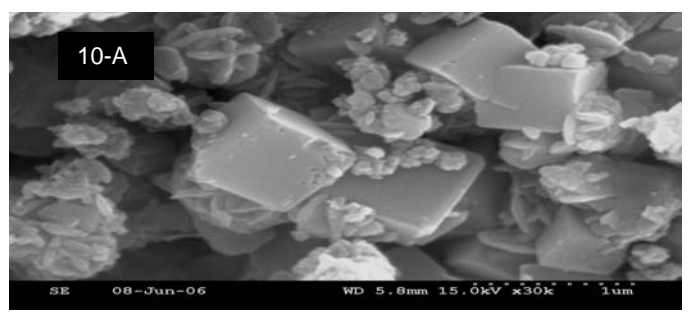


**Fig. 10 Fused ash at 3.5N at 60 °C. Zeolite A formation at different crystallization periods. A) 6 hours B) 24 hours and C) 72 hours.**

#### 4.4 MECHANISM OF ZEOLITE A FORMATION

Zeolite A did form in significant amounts and its formation was reproducible and positively affected the CEC value of the total produced zeolitic materials. This section will focus on zeolite A percentages and contribution to the final cation exchange capacity of the treated ash as well as the morphology and the physical characteristics of the formed zeolite A. Figures 11 and 12 show the estimated percentages and the CEC values for zeolite A formation, respectively. The figures present percentage or CEC values versus fused ash at 1.5N, 2.5N and 3.5N for 60 °C and 100 °C temperatures at 6, 24 and 72 hours curing periods. As shown in Figure 11, under all conditions studied, it was found that zeolite A yields was highest for 2.5N fused ash reaction, similar results obtained by Myake et. al., 2002. It was also found that as the temperature increases, reaction time should be reduced to obtain higher yield of zeolite A. The correlation between the percentages of zeolite A formation and the CEC values can be clearly seen in figures 11 and 12.

It was also found that for the ash that was treated hydrothermally at 100 °C, fusion at 1.5N was not enough to activate silica and alumina in the ash particles. This was confirmed by the precipitation of alumina added to the reaction system in the form of alumina hydroxide. On the other hand, as the ash was fused at 2.5N and 3.5N, zeolite A was formed in significant amounts with optimum results obtained at 2.5N. The increase in zeolitic materials formation when fusing the ash at 2.5N indicated that increasing the hydroxide content resulted in the dissolution of more silica and made it available for reaction. Zeolite A formation was always occurred when silica/alumina ratio was reduced. This confirms that the silica/alumina ratio of the original ash, 13.9, was high and not suitable for zeolite A formation, this finding is of importance since it provides key for controlling and optimization the process of zeolite A formation. The reduction in zeolitic materials formation as hydroxide content was increased by fusing the ash at 3.5N resulted from hydroxyl attack to Al-O-Al bridges in zeolite A structure. It was found that reaction time is important for zeolite A formation, and in this particular study and at the used conditions it was found that 6 hours seems to be the best for zeolite A formation for ash treated at 100 °C. Finally, zeolite of sodalite structure was found to form when the fused ash was treated at 100 °C which was indicative that the used temperature was high which resulted in rapid dissolution of zeolite A at high alkalinity and resulted in the formation of sodalite structure instead. Therefore, the hydrothermal temperature was reduced from 100 °C to 60 °C. As the hydrothermal reaction temperature was reduced from 100°C down to 60°C, an increase in zeolite A formation was observed when silica/alumina ratio was reduced. As silica/alumina ratio was reduced to 2.5N, zeolite A formed at higher percentages at 60°C than it did at 100°C and it was more stable at the lower temperature. However, at 1.5N fusion zeolite A percentages were still very low, 3.79- 7.86 %, and therefore their contribution to the CEC was negligible.

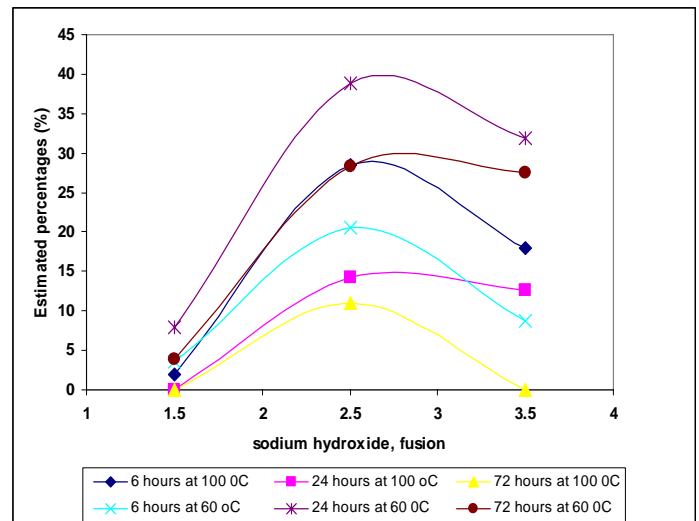


**Fig. 11 Zeolite A percentages that were formed at 1.5N, 2.5N and 3.5N fused ash for hydrothermal treatment at 60 °C and 100 °C for 6, 24 and 72 hours**

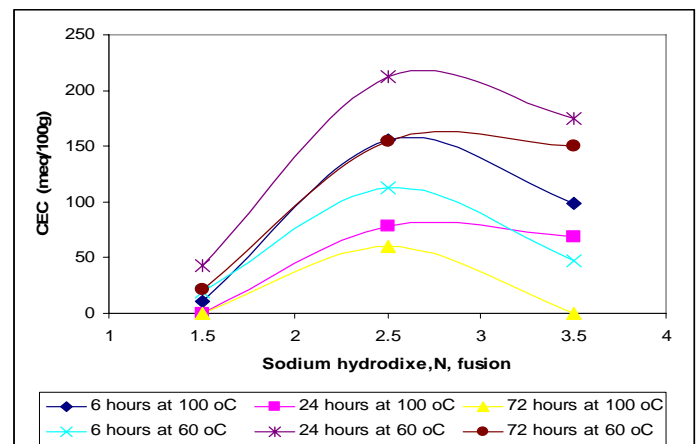


**Fig. 12 The CEC values for zeolite A obtained at different treatments of 1.5N, 2.5N and 3.5N fused ash for hydrothermal treatment at 60 °C and 100 °C for 6, 24 and 72 hours.**

These results were expected since at 1.5N, the silica in the ash particles is not active as concluded from the results observed at 100 °C. This also was confirmed by the precipitation of excess alumina added to the reaction. SEM images for fused ash at 1.5N at 60°C showed that zeolite A crystal sizes were small, in the range of 0.5-0.62 μm, this could be due to the lack of active silica in the ash at these conditions, which resulted in limiting the growth of zeolite A crystals.

On the other hand, as the fused ash was treated at 2.5N and at silica/alumina ratio of 2.5, zeolite A was formed in significant amounts, 20.6-38.8%, and the CEC of zeolite A were high, 112.7-212.8 meq/100g. It was found that the optimum condition for zeolite A formation was at 24 hours, this was not the case when the reaction temperature was 100°C where the optimum

time was 6 hours. As the reaction temperature decreased, time should be increased to allow crystals to grow. SEM images showed that zeolite A crystals formed for fused ash at 2.5N at 60°C has the largest crystals sizes, 1.1-1.6 µm, observed during the present study. The larger crystal sizes obtained in this case indicate that treating the ash at 60°C is more favorable for zeolite A formation than treatment at 100°C though it required more time for crystal growth. These results are expected since zeolites of low density and high volume, such as zeolite A, require low energy to form and they tend to transform into denser zeolites such as sodalite.

The present study concluded that there are two possible theories for zeolite A formation. First, it is possible that zeolite A nuclei formation was triggered by the formation of D4R sub unit in the solution first by interaction between the added aluminates and the formed sodium silicate. These subunits react with sodalite cages, formed in the gel phase, to build zeolite A structure. The second theory is that zeolite A nuclei were formed solely in solution as sodium silicates reacted spontaneously with the added aluminates to form nuclei of zeolite A. the nuclei continue their growth by consuming nutrients from the gel phase or the solution phase. It was not possible to know for sure which path was taken by zeolite A in its formation, but it can be said that the formation of sodium silicate within the gel and the addition of sodium aluminates were key factors for initiating nuclei for zeolite A to form. So in the present study it can be concluded that mechanism of zeolite A formation is considered as solution transport mediated process that involved both gel and solution interaction rather than being pure solution reaction or pure gel transformation process. Figure 13 shows schematic presentation for possible paths for zeolite A formation.

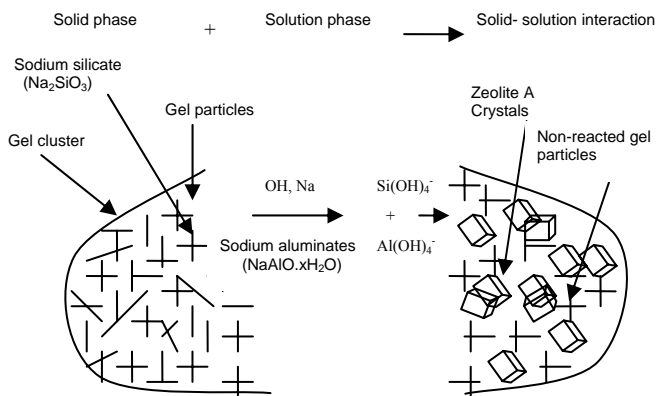


**Fig. 13 Schematic presentations for zeolite A formation process.**

## CONCLUSION

Applying fusion and hydrothermal treatment successfully produced zeolite A from municipal solid waste ash. Fusing MSW ash prior to hydrothermal treatment has dramatically changed both physical and chemical properties of the ash and

resulted in the formation of sodium alumina silicates and sodium silicates precursors to zeolites A. Both amounts and the cation exchange capacity of the ash were increased significantly. Adjusting SiO<sub>2</sub>/Al<sub>2</sub>O<sub>3</sub> was found to be decisive for zeolite A formation. The formation of sodium silicate within the gel and the addition of sodium aluminates were key factors for initiating nuclei for zeolite A to form. The mechanism of zeolite A formation is considered as solution transport mediated process that involved both gel and solution interaction rather than being pure solution reaction or pure gel transformation process. Solution super saturation and optimum silica/alumina ratio were the driving force for nucleation of zeolite A.

The cation exchange capacity of the ash material increased from 17 meq/100g up to 212 meq/100g. The increase in the cation exchange capacity due to zeolite formation increased the potential of using this zeolitic material as adsorbents for both industrial and environmental purposes. The present work sets the bases and fundamentals of zeolite synthesis from MSW ash. By conducting more research work based on the finding of the present study to improve and better understand zeolite formation from MSW ash, it will be possible to introduce such zeolitic materials to the market for commercial uses as adsorbents.

## REFERENCES

- Bosnar S. and Subotic B., 1999. Microporous and Mesoporous Materials, 28: p483.
- Feoktistova N. N Zhdanov and S. P., 1996. Russian Chemical Bulletin, 45: p2287.
- Miyake M., tamura C., and Mastuda M., 2002. J. Am. Ceram. Soc., 85: p1873.
- Molina, A. and Poole, C., 2004. A comparative study using two methods to produce zeolites from fly ash. Minerals Engineering, 17:p167-173.
- Murayama, N., Tanabe, M., Yamamoto, H. and Shibata, J., 2002. Mechanism of zeolite synthesis from coal fly ash by alkali hydrothermal reaction. International Journal of Mineral Processing, 64: p1-17.
- Murayama, N., Tanabe, M., Yamamoto, H. and Shibata, J., 2003. Reaction, mechanism and application of various zeolite syntheses from coal fly ash. Materials transactions, 44(12):p2475-2480.
- Polak F.,1971. International Chemical Engineering, 11:p439.
- Yamazaki S. and Tsutumi K., 2000. Microporous and Mesoporous Materials, 37: p67.